exothermic decomposition of NC gives off products such as solid carbon along with the gaseous ones. This may be the reason for the observation of carbon particles on the burning surface by Heath and Hirst.[4] They also observed a number of globules on the surface that they attributed to gas bubbles. These globules may be NG and other volatile components of DBP leaving the surface.

In view of the above discussion, it is appropriate to say that NC first decomposes on the surface exothermically and NG boils, vaporizes, and finally diffuses out of the surface. The decomposition of NC is too fast and hence cannot control the surface regression reactions. It is likely that NG diffusion, being the slower step, may be the rate-controlling step. These decomposed products of NC and the vaporized NG along with other volatiles may react and produce heat in the fizz zone.

Conclusions

The large amount of heat required for double-base propellant regression may be caused by the exothermic heat released during NC decomposition in the condensed phase.

During low-temperature decomposition of the DBP, NG undergoes diffusional vaporization and leaves behind a decomposed propellant richer in NC.[5] On the other hand, during burning NC decomposes and leaves the burning surface richer in NG. It may be said that since NC primarily governs the propellant regression, burning rate modifications could be effectively carried out by those methods that bring about changes in the thermal decomposition behavior of NC.

References

[1] Kishore, K., Pai Verneker, V. R., Chaturvedi, B. K., and Gayathri, V., "Mechanistic Studies on Composite Solid Propellants," *AIAA Journal*, Vol. 15, Jan. 1977, pp. 114-116.

[2] Kishore, K., Pai Verneker, V. R., and Gayathri, V., "Reaction Intermediates during Combustion and Decomposition of Some Model Solid Rocket Fuels," *Fuel*, Vol. 60, Feb. 1981, pp. 164-167.

[3] Pai Verneker, V. R., Kishore, K., and Subhas, C.B.V., "Thermal Reactivity of Double Base Rocket Propellants," *Propellants and Explosives*, Vol. 4, 1979, pp. 83-86.

[4] Heath, G. A. and Hirst, R., "Some Characteristics of the High Pressure Combustion of Double-Base Propellants," *Eighth Symposium (International) on Combustion*, Williams and Wilkins Co., Baltimore, Md., 1960, pp. 711-719.

[5] Pai Verneker, V. R., Kishore, K., and Subhas, C.B.V., "Comparative Assessment of the Thermal Decomposition and Combustion Behavior in Double Base and Composite Solid Propellants," *AIAA Journal*, to be published.

Stability of Annular Sector Plates with Variable Thickness

R. S. Srinivasan* and V. Thiruvenkatachari†
Indian Institute of Technology, Madras, India

Introduction

ALTHOUGH many researchers have studied the buckling of circular and annular plates, the only reference available on the stability of annular sector plates is that of Rubin.[1] Rubin has considered a plate with simply supported radial edges with arbitrary boundary conditions along curved edges. The plate is subjected to constant in-plane forces along the radial and circumferential directions.

In this Note the stability analysis of a clamped annular sector plate with variable thickness subjected to uniform load along the radial direction is presented. A numerical method using matrix algebra, which had been adopted earlier for the study of buckling of skew plates,[2] has been used.

Received Nov. 29, 1982.

*Professor, Department of Applied Mechanics.
†Research Scholar, Department of Applied Mechanics.

Differential Equations

Consideration of the equilibrium of the plate shown in Fig. 1 results in

$$\frac{\partial}{\partial r}(rM_r)+\frac{\partial}{\partial \theta}(M_{r\theta})-M_\theta-rQ_r=0 \tag{1}$$

$$\frac{\partial}{\partial r}(rM_{r\theta})+\frac{\partial}{\partial \theta}(M_\theta)+M_{r\theta}-rQ_\theta=0 \tag{2}$$

$$\frac{\partial}{\partial r}\left[rN_r\frac{\partial w}{\partial r}+N_{r\theta}\frac{\partial w}{\partial \theta}+rQ_r\right]$$
$$+\frac{\partial}{\partial \theta}\left[\frac{1}{r}N_\theta\frac{\partial w}{\partial \theta}+N_{r\theta}\frac{\partial w}{\partial \theta}+Q_\theta\right]=0 \tag{3}$$

$$\frac{\partial}{\partial r}(rN_r)+\frac{\partial}{\partial \theta}(N_{r\theta})-N_\theta=0 \tag{4}$$

$$\frac{\partial}{\partial r}(rN_{r\theta})+\frac{\partial}{\partial \theta}(N_\theta)+N_{r\theta}=0 \tag{5}$$

The boundary conditions are

at

$$r=a,\quad N_r=\frac{P}{a\theta_0},\quad N_{r\theta}=w=\frac{\partial w}{\partial r}=0 \tag{6a}$$

$$r=b,\quad N_r=\frac{P}{b\theta_0},\quad N_{r\theta}=w=\frac{\partial w}{\partial r}=0 \tag{6b}$$

$$\theta=0 \text{ and } \theta_0,\quad N_\theta=N_{r\theta}=w=\frac{\partial w}{\partial \theta}=0 \tag{6c}$$

where P is the total load applied uniformly on a curved edge.

The solution of Eqs. (4) and (5) subjected to the in-plane boundary condition mentioned in Eqs. (6) can be written from Ref. 3 as

$$N_r=-\frac{2P\cos(-\theta_0/2+\theta)}{r(\theta_0+\sin\theta_0)},\quad N_\theta=N_{r\theta}=0 \tag{7}$$

Using Eqs. (1-3) and noting that the rigidity of the plate is not constant, the governing differential equation can be written as

$$\nabla^2(D\nabla^2 w)-(1-\mu)\left[\frac{\partial^2 D}{\partial r^2}\left(\frac{1}{r}\frac{\partial w}{\partial r}+\frac{1}{r^2}\frac{\partial^2 w}{\partial \theta^2}\right)-2\frac{\partial}{\partial r}\left(\frac{1}{r}\frac{\partial D}{\partial \theta}\right)\right.$$
$$\left.\times\frac{\partial}{\partial r}\left(\frac{1}{r}\frac{\partial w}{\partial \theta}\right)+\frac{\partial^2 w}{\partial r^2}\left(\frac{1}{r}\frac{\partial D}{\partial r}+\frac{1}{r^2}\frac{\partial^2 D}{\partial \theta^2}\right)\right]=N_r\frac{\partial^2 w}{\partial r^2} \tag{8}$$

where

$$\nabla^2=\left(\frac{\partial^2}{\partial r^2}+\frac{1}{r}\frac{\partial}{\partial r}+\frac{1}{r^2}\frac{\partial^2}{\partial \theta^2}\right)$$

and

$$D=\frac{Eh^3}{12(1-\mu^2)}$$

and μ is Poisson's ratio.

Taking the thickness variation as (see Fig. 1)

$$h=h_0\{1+[\bar{r}-(b/c)]\eta\}=h_0H(\bar{r}) \tag{9}$$

and using Eqs. (7) and (9), Eq. (8) can be written in nondimensional form as

$$\left[\bar r^4\frac{\partial^4 w}{\partial\bar r^4}+\bar r\frac{\partial w}{\partial\bar r}-\bar r^2\frac{\partial^2 w}{\partial\bar r^2}+2\bar r^3\frac{\partial^3 w}{\partial\bar r^3}+\frac{4}{\theta_0^2}\frac{\partial^2 w}{\partial\bar\theta^2}\right.$$
$$\left.-\frac{2}{\theta_0^2}\bar r\frac{\partial^3 w}{\partial\bar r\delta\bar\theta^2}+\frac{2}{\theta_0^2}\frac{\partial^4 w}{\partial\bar r^2\partial\bar\theta^2}+\frac{1}{\theta_0^4}\frac{\partial^4 w}{\partial\bar\theta^4}\right]+\frac{3\eta}{[H(\bar r)]}\left[2\bar r^3\frac{\partial^2 w}{\partial\bar r^2}\right.$$
$$\left.+2\bar r^4\frac{\partial^3 w}{\partial\bar r^3}+\mu\bar r^3\frac{\partial^2 w}{\partial\bar r^2}-\bar r^2\frac{\partial w}{\partial\bar r}-\frac{3}{\theta_0^2}\frac{\partial^2 w}{\partial\bar\theta^2}+\frac{2}{\theta_0^2}\bar r^2\frac{\partial^3 w}{\partial\bar r\partial\bar\theta^2}\right]$$
$$+\frac{6\eta^2}{[H(\bar r)]^2}\left[\bar r^4\frac{\partial^2 w}{\partial\bar r^2}+\mu\bar r^3\frac{\partial w}{\partial\bar r}+\frac{\mu}{\theta_0^2}\bar r^2\frac{\partial^2 w}{\partial\bar\theta^2}\right]$$
$$=\lambda\bar r^3\frac{\cos[-(\theta_0/2)+\bar\theta]}{[H(\bar r)]^3}\frac{\partial^2 w}{\partial\bar r^2}\tag{10}$$

where

$$\lambda=\frac{2P[1-(b/a)]a}{D_0(\theta_0+\sin\theta_0)}$$

and

$$D_0=\frac{Eh_0^3}{12(1-\mu^2)},\quad \bar r=\frac{r}{c},\quad \bar\theta=\frac{\theta}{\theta_0}$$

Solution

The annular sector plate is divided by equidistant parallel curved arcs and by radial lines at equal angles (see Fig. 1).

Let

$$\frac{\partial^4 w}{\partial\bar r^4}=k(\bar r,\bar\theta)\tag{11a}$$

and

$$\frac{\partial^4 w}{\partial\bar\theta^4}=\ell(\bar r,\bar\theta)\tag{11b}$$

For a line with $\bar\theta=\bar\theta_n$, Eq. (11a) with boundary conditions (6a) and (6b) can be written as

$$w(\bar r,\bar\theta_n)=\int_0^1 G(\hat r,\hat\xi,\bar\theta_n)\bar k_n(\hat\xi,\bar\theta_n)\,\mathrm{d}\hat\xi\tag{12}$$

where $\hat r=\bar r-(b/c)$, $\hat\xi=\bar\xi-(b/c)$, and $G(\hat r,\hat\xi,\bar\theta_n)$ is Green's function.

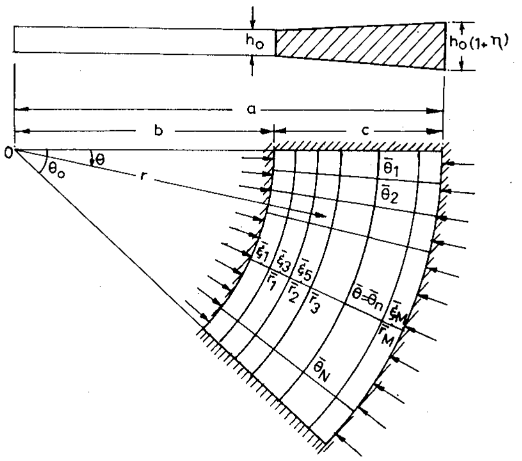

Fig. 1 Annular sector plate.

Using Simpson's rule and parabolic interpolation, Eq. (12) can be written as

$$\{w_n\}=[G_n][\alpha][S]\{k_n\}=[A_n]\{k_n\}\tag{13}$$

where $[\alpha]$ is the matrix containing the coefficients of Simpson's rule and $[S]$ the interpolation matrix.

Writing the expressions similar to Eq. (13) for other lines and combining them, the final equation is written as

$$\{w\}=[A]\{k\}\tag{14}$$

For all lines in the θ direction, the corresponding expression using Eq. (11b) is written as

$$\{w^*\}=[B]\{\ell^*\}\tag{15}$$

The order of the points considered in $\{w^*\}$ in the above equation is different from that in $\{w\}$. By a suitable transformation one can write

$$\{w\}=[\tilde B]\{\ell\}\tag{16}$$

From Eqs. (14) and (16) the derivatives can be written as

$$\{w'\}=[A'][A]^{-1}[\tilde B]\{\ell\},\quad \{w^0\}=[\tilde B^0]\{\ell\},$$
$$\{w^{0\prime}\}=[A'][A]^{-1}[\tilde B^0]\{\ell\}\tag{17}$$

where superscript primes and zeros denote differentiation with respect to $\bar r$ and $\bar\theta$, respectively. Substituting these expressions in Eq. (10) one obtains

$$[\ulcorner\bar r^4\lrcorner][A]^{-1}[\tilde B]\{\ell\}+[\ulcorner\bar r\lrcorner][A'][A]^{-1}[\tilde B]\{\ell\}$$
$$-[\ulcorner\bar r^2\lrcorner][A''][A]^{-1}[\tilde B]\{\ell\}+2[\ulcorner\bar r^3\lrcorner][A'''][A]^{-1}[\tilde B]\{\ell\}$$
$$+C_1[\tilde B^{00}]\{\ell\}-C_2[\ulcorner\bar r\lrcorner][A'][A]^{-1}[\tilde B^{00}]\{\ell\}$$
$$+C_2[A''][A]^{-1}[\tilde B^{00}]\{\ell\}+C_3[\,I\,]\{\ell\}$$
$$+[\ulcorner F_1\lrcorner](2[\ulcorner\bar r^3\lrcorner][A''][A]^{-1}[\tilde B]\{\ell\}$$
$$+2[\ulcorner\bar r^4\lrcorner][A'''][A]^{-1}[\tilde B]\{\ell\}+C_4[\ulcorner\bar r^3\lrcorner][A''][A]^{-1}[\tilde B]\{\ell\}$$
$$-[\ulcorner\bar r^2\lrcorner][A'][A]^{-1}[\tilde B]\{\ell\}+C_5[\tilde B^{00}]\{\ell\}$$
$$+C_2[\ulcorner\bar r^2\lrcorner][A'][A]^{-1}[\tilde B^{00}]\{\ell\})+[\ulcorner F_2\lrcorner]([\ulcorner\bar r^4\lrcorner][A''][A]^{-1}[\tilde B]\{\ell\}$$
$$+C_4[\ulcorner\bar r^3\lrcorner][A'][A]^{-1}[\tilde B]\{\ell\}+C_6[\ulcorner\bar r^2\lrcorner][\tilde B^{00}]\{\ell\})$$
$$=\lambda[\ulcorner F_3\lrcorner][\ulcorner\bar r^3\lrcorner][A''][A]^{-1}[\tilde B]\{\ell\}\tag{18}$$

where

$$\varphi=1/\theta_0^2,\quad C_1=4\varphi,\quad C_2=2\varphi,\quad C_3=\varphi^2,\quad C_4=\mu,$$
$$C_5=-3\varphi,\quad C_6=\mu\varphi,\quad F_1=3\eta/H(\bar r),\quad F_2=6\eta^2/[H(\bar r)]^2$$
$$F_3=\cos\left(-\frac{\theta_0}{2}+\bar\theta\right)\Big/[H(\bar r)]^3$$

Equation (18) can be written as

$$[K]\{\ell\}=\lambda[S]\{\ell\}\tag{19}$$

The buckling load is obtained by solving this eigenvalue problem.

Numerical Work

A study of the convergence of the buckling load was made for a plate with $\theta_0=60$ deg, $(b/a)=0.5$, and $\eta=0.3$. The values of buckling load parameter λ for 5×5, 7×7, 9×9, and

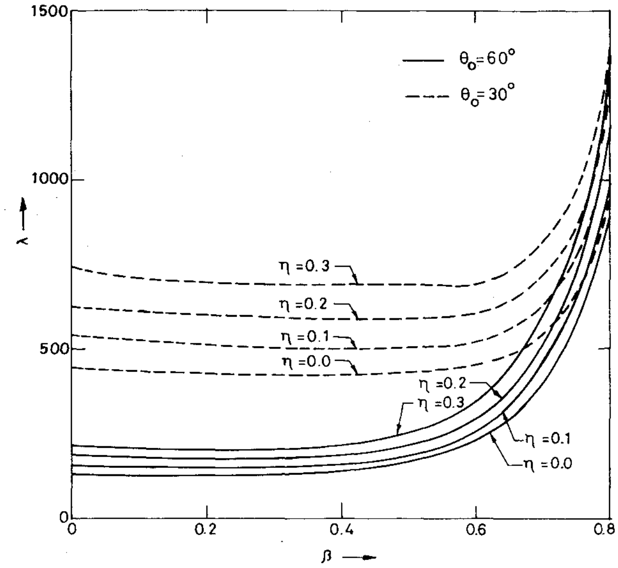

Fig. 2 Variation of stability coefficient vs radii ratio.

11×11 meshes are found to be 123.9, 122.8, 122.0, and 121.6, respectively. It is found that 9×9 mesh gives good convergence. The same mesh size has been adopted for further work and Poisson's ratio was 0.3.

Since no other results are available for comparison the annular sector plate is approximated to a square plate of constant thickness using $\theta_0 = 1.14$ deg, $b = 50.0$, and $\eta = 0$. The buckling parameter is found to be 4915, which compares well with the value of 5000 given by Levy (see Ref. 4).

A parametric study has been made varying the radii ratio β $(= b/a)$ from 0 to 0.8, the thickness parameter η from 0 to 0.3 for the sector plate angles (θ_0) of 30, 60, 90, and 120 deg. Typical results for $\theta_0 = 30$ and 60 deg are presented in Fig. 2.

It can be observed from Fig. 2 that for any annular sector plate of θ_0, if the radii ratio β is increased the critical load remains constant up to a certain value of β and then increases monotonically. It is also found that the critical load decreases as θ_0 is increased.

References

[1] Rubin, C., "Stability of Polar Orthotropic Sector Plates," *Journal of Applied Mechanics, Transactions of ASME*, Vol. 45, 1978, pp. 448-450.

[2] Srinivasan, R. S. and Ramachandran, S. V., "Stability of Clamped Skew Plates," *Journal of Structures Division, Proceedings of ASCE*, Vol. 102, 1976, pp. 569-574.

[3] Timoshenko, S. and Goodier, G. N., *Theory of Elasticity*, McGraw Hill Book Co., London, 1951.

[4] Bulson, P. S., *The Stability of Flat Plates*, Chatto and Windus Co., London, 1970.

Radiative Heat Transfer in Segregated Media

R. K. Ahluwalia* and K. H. Im*
Argonne National Laboratory, Argonne, Illinois

Nomenclature

h = enthalpy
I_b = black-body intensity
I_w = I_b at wall temperature
k_{eff} = effective thermal conductivity
n = particle size distribution function
p = pressure
Q = heat flux
R = radius
r,x = radial and axial coordinates, respectively
r_p = radius of the particle
T = temperature
u,v = axial and radial velocities, respectively
β = extinction coefficient
ϵ_w = wall emissivity
μ_{eff} = effective viscosity
ν = frequency
ρ = density
ω = scattering albedo

Received Oct. 15, 1982; revision submitted May 20, 1983.

*Mechanical Engineer, Engineering Division.

Introduction

THE problem of heat transfer in particle-laden flows is important in many engineering applications, such as pulverized coal combustors, oil combustors, solid propellant rocket nozzles, diffuser and radiant boilers of coal-fired magnetohydrodynamic plants, and nuclear reactors. In some of these applications a particular problem of heat transfer in a segregated medium is encountered. For instance, in a coal-burning swirl combustor the coal particles may be segregated in the core region near the injection point, and in the wall region further downstream. A question then arises as to how the stratification of a large number of absorbing (and emitting) and scattering particles influence the heat-transfer characteristics of the medium. In a previous study[1] this question was investigated by formulating a radiative heat-transfer model for a cylindrical absorbing-emitting-scattering medium, idealized to consist of two regions possessing uniform but different spectral properties. In other words, the radiation properties were assumed to suffer a step change at the interface of the two regions. An important conclusion of the study was that the segregation of particles can have a significant influence on the heat-transfer rate. A large number of particles in the highly emitting core region can enhance the heat flux inasmuch as the segregation of particles in the highly absorbing wall region can diminish the heat-transfer rate by an order of magnitude.

This Note deals with an extension of analysis conducted in Ref. 1. The restrictive assumption of the spectral properties changing discontinuously across the boundary between the two regions is relaxed. Instead, the spectral properties are considered to vary in any arbitrary and continuous fashion. In order to investigate specifically the influence of segregation of

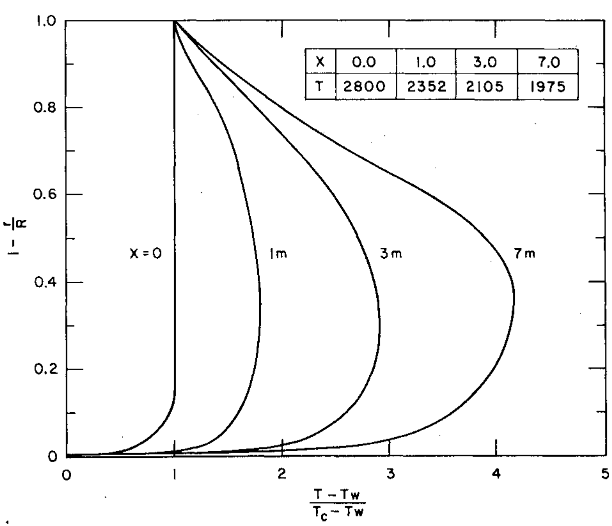

Fig. 1 Development of temperature profile with particles concentrated in the core.